Journal of
Synchrotron Radiation

ISSN 0909-0495

Received 4 February 2011
Accepted 14 June 2011

Carbon contamination of soft X-ray beamlines: dramatic anti-reflection coating effects observed in the 1 keV photon energy region

C. Chauvet, F. Polack, M. G. Silly, B. Lagarde, M. Thomasset, S. Kubsky, J. P. Duval, P. Risterucci, B. Pilette, I. Yao, N. Bergeard and F. Sirotti*

Synchrotron Soleil, L'Orme des Merisiers, Saint Aubin, 91193 Gif sur Yvette, France.
E-mail: fausto.sirotti@synchrotron-soleil.fr

Carbon contamination is a general problem of under-vacuum optics submitted to high fluence. In soft X-ray beamlines carbon deposit on optics is known to absorb and scatter radiation close to the C *K*-edge (280 eV), forbidding effective measurements in this spectral region. Here the observation of strong reflectivity losses is reported related to carbon deposition at much higher energies around 1000 eV, where carbon absorptivity is small. It is shown that the observed effect can be modelled as a destructive interference from a homogeneous carbon thin film.

Keywords: carbon contamination; beamline optics; X-ray reflectivity; optical thin film.

1. Introduction

Since first experiments using soft X-ray synchrotron radiation, carbon contamination of optics has been observed and studied to determine the structure of the carbon layer. In 1980 it was shown that intensity modulations in X-ray absorption spectra, caused by carbon contamination on Au and Pt mirror surfaces exposed to high-intensity synchrotron radiation, are closely similar to the near C *K*-edge absorption spectrum of bulk crystalline graphite (Denley *et al.*, 1980). This indicated the formations of graphitic overlayers on such mirrors even under ultrahigh-vacuum conditions. Several procedures have been developed to clean the optical elements at all the synchrotron radiation centres (Johnson *et al.*, 1987; Kita *et al.*, 1992; Harada *et al.*, 1991; Eggstein *et al.*, 2001), but carbon contamination remains a major problem for soft X-ray beamlines.

At SOLEIL we have observed a high carbon deposition rate on all beamlines in the VUV and the soft X-ray region resulting in thick carbon layers deposited on the beamline optics. In the following we present modifications of the TEMPO beamline transmission induced by the carbon contamination of the first optical element of the beamline during the first years of operation.

2. Mirror contamination at the TEMPO beamline

TEMPO is a soft X-ray beamline dedicated to time-dependent photoelectron spectroscopy experiments of the SOLEIL synchrotron radiation source of 2.75 GeV. The energy range of the beamline was optimized for the region between 40 eV and 1500 eV to perform X-ray absorption, soft X-ray photoemission and angular-resolved photoemission experiments on metal and semiconductor samples. The main research topics are related to the study of surface magnetic properties and surface chemical reactions.

The soft X-ray photons are produced by two Apple II type insertion devices with periods of 80 mm and 44 mm (Diviacco *et al.*, 2005). The photon flux emitted by the insertion devices is delimited by a sizable water-cooled aperture. The accepted beam is reflected by two mirrors in the horizontal plane before entering a plane-grating spherical-mirror monochromator (Polack *et al.*, 2010). The maximum power emitted through the aperture for both insertion devices is of the order of 250 W. The setting of the insertion devices and the aperture size strongly depend on the specific experiment. On average, the current operation of the beamline is estimated to expose the first optics to a mean power of 100 W.

The two first mirrors of the beamline are hosted in the same UHV chamber with a base pressure of 5×10^{-10} mbar and a maximum pressure of 6×10^{-8} mbar during beam operation. They are cryogenically cooled at 85 K. The residual mass spectrum measured in the chamber while the beam is present is compared in Fig. 1 (red curve) with the mass spectrum measured without photon beam (blue curve). We observe a pressure increase from the low 10^{-10} mbar range to some 10^{-8} mbar pressure with a high amount of carbon. The masses corresponding to C, CO and CO_2 atomic and molecular species are indicated in Fig. 1.

After one year of operation the trace of the direct beam appeared as a black line across the mirrors, and a cleaning operation was applied. A mercury UV lamp was installed a few centimetres in front of each mirror. The chamber was

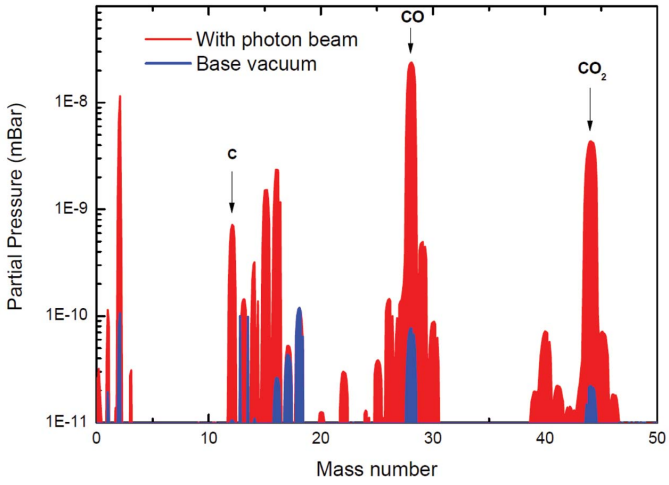

Figure 1
Comparison of the mass spectra measured in the first mirrors chamber with and without the synchrotron radiation beam. The blue curve corresponds to the base vacuum of the chamber; the red one was measured in the presence of a photon beam emitted by the HU80 insertion device. The power received by the first mirror is about 100 W. The masses corresponding to C, CO and CO_2 are indicated in the figure.

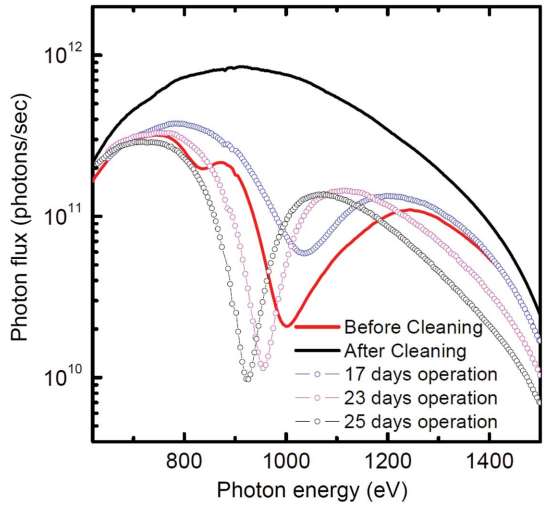

Figure 2
Photon flux measured on the beamline at different dates during the first year of operation. The red spectrum (continuous line) was measured in December 2008 just before the cleaning procedure was applied to the first mirrors. The dramatic transmission reduction observed around 1 keV disappeared after cleaning as shown by the continuous black line. The blue, magenta and black empty dots transmission curves were measured after 17, 23 and 25 days operation, respectively.

filled with 400 mbar of ultra pure oxygen. Then the lamps were turned on and the mirrors were exposed to activated oxygen for about 8 h.

The mirror surface roughness was measured using a phase-shift interferential microscope (Optosurf by Eotech, Marcoussis, France) at delivery time, then before and after the cleaning procedure. A roughness of 1.8 nm r.m.s. was measured at delivery, rising to 3.5 nm r.m.s. before cleaning, and dropping again to 1.6 nm r.m.s. after cleaning. We also recovered the initial mirror reflectivity and the initial beamline transmission.

The spectral transmission of the beamline was measured before and after mirror cleaning, then at regular intervals after cleaning. These measurements are presented in Fig. 2 where the photon flux transmitted by the beamline is plotted *versus* photon energy between 650 eV and 1500 eV. The red curve was recorded before cleaning and the black curve just after cleaning. The black curve presents a maximum transmitted intensity around 900 eV and follows well the calculation performed by the Soleil Optics Group during the beamline design. Curves measured after cleaning clearly show the evolution of mirror reflectivity with increasing carbon contamination thicknesses.

Starting from clean mirror conditions (black curve), a dip in the beamline transmission curve appears around 1000 eV after 17 days of beam exposure (blue curve). This minimum becomes deeper and moves to lower photon energies as a function of the beamline operation time, that is, as a function of the carbon layer thickness. For the thicker layer that was actually present on the mirror at the end of 2008, before the cleaning procedure (red curve), two minima are observed around 850 eV and 1000 eV. The reflectivity dips moving toward larger wavelength with thicker carbon deposit and the observation of multiple minima for larger thickness is a clear indication of a destructive interference effect in the carbon contamination thin film.

3. Reflectivity model and discussion

In order to confirm the origin of the observed behaviour of beamline transmission with increasing contamination, we have calculated the change in reflected intensity from a Pt mirror covered with a carbon layer of increasing thickness. We have used our *CARPEM* code, originally written to compute grating efficiencies (Mirone *et al.*, 1998*a*,*b*). *CARPEM* represents the electric field and dielectric constant at a given depth from the surface by a truncated Fourier series of the in-plane periodicity. The complex reflectivity matrix is computed by solving the Maxwell equations thin layer by thin layer with an *R*-matrix propagation algorithm. For uniform layers, computations simply reduce to the use of one Fourier term in the series.

The contaminated mirror was modelled as a thick Pt surface covered with a carbon layer of variable thickness between 0 and 100 nm. For the 2.15° grazing angle of the soft X-ray beam on the first mirrors the best match of simulated to measured data was found with a carbon layer density equal to 2 g cm^{-3}, slightly smaller than the density of bulk graphite (2.2 g cm^{-3}). Optical constants are those of CXRO.[1]

The calculated reflected intensity is shown in Fig. 3 as a function of the photon energy and for a layer thickness between 0 and 50 nm. This complex diagram can be divided

[1] The Center of X-ray Optics (CXRO) at Berkeley National Laboratory, Berkeley, CA, USA (http://henke.lbl.gov/optical_constants/). A reflectivity calculator is also available at http://henke.lbl.gov/optical_constants/layer2.html and gives the same results as *CARPEM*.

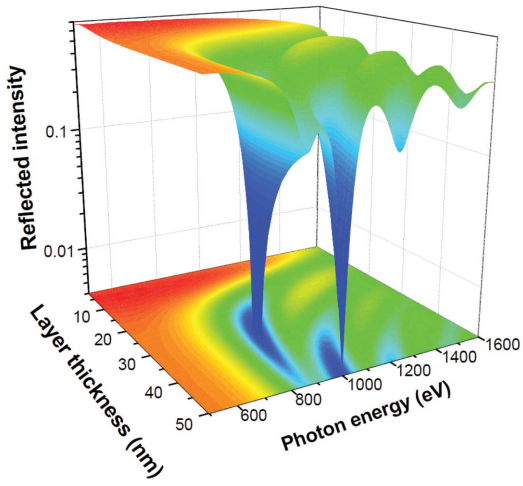

Figure 3
Mirror reflectivity calculated using the *CARPEM* code for a Pt-coated mirror covered by a carbon layer of variable thickness. The reflected intensity at 2.15° grazing incidence is shown as a function of the photon energy and of the layer thickness.

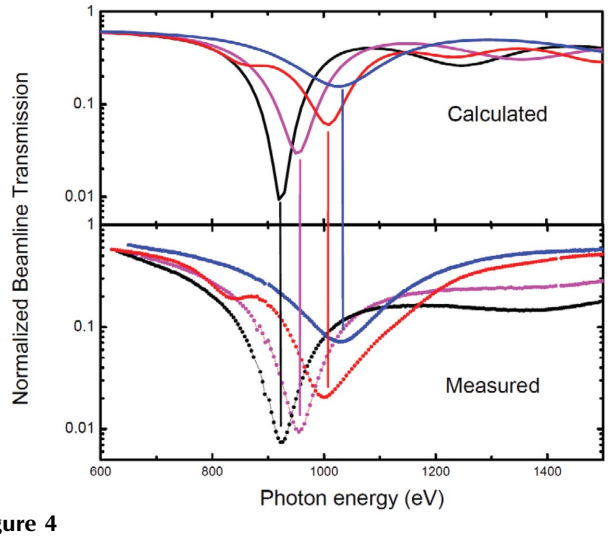

Figure 4
Comparison between the calculated (top panel) and the measured (bottom panel) transmission curves, normalized to clean mirror conditions. The calculated curves were obtained for carbon layers of thickness 20 nm (blue), 26 nm (magenta), 30 nm (black) and 50 nm (red). The measured transmission curves (bottom panel) were obtained after 17, 23, 25 and 50 days operation (indicated by blue, magenta, black and red data points, respectively).

into two energy regions where the reflectivity at the top carbon layer has different behaviours. The transition energy, called the critical energy in the following, is that for which the grazing-incidence angle is equal to the critical angle for total external reflection of carbon. This critical energy is 790 eV in our 2.15° grazing-angle conditions. For energies lower than the critical energy, the grazing incidence angle is smaller than the critical angle and only evanescent waves propagate in the carbon layer. The reflectivity is hence almost insensitive to the carbon layer thickness but for the smallest thicknesses where a fraction of the incident energy can still reach the platinum surface. Above the critical energy the grazing-incidence angle is larger than the critical angle, and a transmitted wave can propagate through the carbon layer and reach the platinum surface, where it is reflected back and hence interferes with the wave reflected at the carbon surface. The contrast of this interference depends on the intensity match between the two waves. It is maximal close to the critical energy where almost complete extinction can be observed for some thicknesses, then vanishes at higher energies with the fading out of reflectivity from the carbon surface. The positions of minima and maxima are related to the carbon layer thickness and phase shifts at the interfaces.

As a result, the effect of carbon deposition on beamline transmission can be described as follows. A relative minimum of reflectivity appears near 1500 eV when thickness reaches about 10 nm. Then with increasing carbon thickness, this minimum moves toward lower energies and deepens while an overall decrease of reflectivity centered around the critical energy is observed. The reflectivity loss reaches a maximum depth at 900 eV for a thickness of about 25 nm, then slowly fills up before reaching the critical energy (790 eV) while new minima appear at higher energies and deepen as they move to lower ones. For a 50 nm carbon thickness, the second minimum, located at 1 keV, is deeply marked while the first and higher-order minima remain weak.

Selected curves from the calculations of Fig. 3 are compared in Fig. 4 with the measured transmission of the mirrors. The experimental curves (shown in the bottom panel of Fig. 4) are obtained by dividing the transmission of the carbon contaminated mirror of Fig. 2 by the transmission measured for the clean mirror. The resulting curve can now be compared directly with the normalized calculated reflectivity of the carbon-covered mirror extracted from Fig. 3.

In the top panel of Fig. 4 we present the calculated curves obtained for 20, 26, 30 and 50 nm-thick carbon layers. They reproduce the photon energy position of the minima and the observed reduction of the transmitted intensity. The agreement we obtain between measured and calculated curves is excellent. The blurring of the higher interference orders may indicate a slight dispersion of carbon thicknesses over the illuminated surface. However, it witnesses a remarkable uniformity of carbon growth over the whole mirror surface.

4. Conclusion

We have shown how carbon contamination can strongly affect the photon transmission at photon energies higher than the carbon edge. Strong oscillations of the reflectivity *versus* energy can be observed between 800 and 1500 eV, depending on the carbon layer thickness and the incidence angle. These oscillations, which are only observed for incidence angles larger than the critical angle of reflection of carbon, are unambiguously related to interference effects in the contamination film. The reflectivity loss can locally reach two orders of magnitude. The measured reduction of the photon flux of the beamline, normalized to the transmission of the clean optics, is in excellent agreement with optical reflectivity model

calculations. These results illustrate the crucial need for *in situ* cleaning procedures of beamline optics.

References

Denley, D., Perfetti, P., Williams, R. S., Shirley, D. A. & Stöhr, J. (1980). *Phys Rev. B*, **21**, 2267–2273.

Diviacco, B., Bracco, R., Knapic, C., Millo, D., Zangrando, D., Chubar, O., Dael, A., Massal, M. & Martí, Z. (2005). *Proceedings of 2005 Particle Accelerator Conference*, Knoxville, TN, USA, p. 4242.

Eggenstein, F., Senf, F., Zeschke, T. & Gudat, W. (2001). *Nucl. Instrum. Methods Phys. Res. A*, **467–468**, 325–328.

Harada, T., Yamaguchi, S., Itou, M., Mitani, S., Maezawa, H., Mikuni, A., Okamoto, W. & Yamaoka, H. (1991). *Appl. Opt.* **30**, 1165–1168.

Johnson, E. D., Hulbert, S. L., Garret, R. F., Williams, G. P. & Knotek, M. L. (1987). *Rev. Sci. Instrum.* **58**, 1042–1045.

Kita, T., Harada, T., Maezawa, H., Muramatsu, Y. & Namba, H. (1992). *Rev. Sci. Instrum.* **63**, 1424–1427.

Mirone, A., Delcamp, E., Idir, M., Cauchon, G., Polack, F., Dhez, P. & Bizeuil, C. (1998*a*). *Appl. Opt.* **37**, 5816–5822.

Mirone, A., Polack, F., Delcamp, E., Idir, M., Cauchon, G. & Dhez, P. (1998*b*). *Proc. SPIE*, **3450**, 36–43.

Polack, F., Silly, M., Chauvet, C., Lagarde, B., Bergeard, N., Izquierdo, M., Chubar, O., Krizmancic, D., Ribbens, M., Duval, J. P., Basset, C., Kubsky, S. & Sirotti, F. (2010). *AIP Conf. Proc.* **1234**, 185–188.